STUDY ON ELECTROMECHANICAL COUPLING COEFFICIENTS OF SURFACE ACOUSTIC WAVES IN LAYERED SYSTEMS

Yung-Yu Chen, Jin-Cheng Hsu, and Tsung-Tsong Wu*

ABSTRACT

The aim of this paper is to utilize the effective permittivity approach to calculate the electromechanical coupling coefficients of surface acoustic waves in layered systems. The effective permittivity offers a direct relation to the voltage-induced charge density at the interface, and can be used to calculate the phase velocity dispersion and the electromechanical coupling coefficients of a layered piezoelectric medium exactly. In this paper, the formulation based on the matrix method for calculating the effective permittivity of a layered piezoelectric medium with three types of electrode arrangements is given first. Then, based on this formulation, we calculated phase velocity dispersions of the generalized SAW mode and the HVPSAW mode in layered systems of ZnO/Diamond and $LiNbO_3$/Diamond. In addition, the electromechanical coupling coefficients of surface acoustic waves in the aforementioned layered systems with three different electrical boundary conditions were analyzed and discussed.

Key Words: effective permittivity, electromechanical coupling coefficient.

I. INTRODUCTION

Surface acoustic wave (SAW) devices have been applied successfully in various communication systems for many decades. Recently, due to the rapid development of modern communication systems, the requirement for increasing the frequency of a surface acoustic wave filter has led to research in dispersive SAW devices. Among all the known materials, diamond has the highest acoustic wave velocity. By including a diamond layer in a layered structure, the surface wave velocity can be increased significantly (Yamanouchi *et al.*, 1989; Nakahata *et al.*, 1994). This leads to an increase of the SAW frequency without decreasing the electrode spacing in the sub-micron region. In addition, layered SAW devices also preserve the advantages of high coupling coefficient and tiny temperature coefficient (Nakahata *et al.*, 1998).

The electromechanical coupling coefficient is defined as the transformation ratio between the mechanical and electrical energy. It affects insertion loss and bandwidth of the frequency response of a SAW device and plays an important role in the design of a SAW device. Besides, the electromechanical coupling coefficients of a layered structure are frequency dependent, and therefore, the corresponding dispersion analysis becomes an important issue for designing a diamond layered SAW device. In the last decade, there have been experimental as well as theoretical investigations of layered SAW devices including a diamond substrate. In a theoretical calculation, Adler (1990; 1994) presented a matrix approach for studying SAW and pseudo SAW in layered piezoelectric media. Later, based on the matrix method, Adler and Solie (1995) calculated the electromechanical coupling of layered SAW with ZnO on Diamond. In a calculations, different boundary conditions were considered. By using the conventional approach for calculating surface wave dispersion, Nakahata *et al.* (1995) reported analyses of phase velocity and electromechanical coupling coefficient for three different layered SAWs with diamond as the middle layer. In a subsequent paper, Nakahata *et al.* (1995) also reported experimental results on a 2.5 GHz SAW fil-

*Corresponding author. (Fax: 886-2-33665663; Email: wutt@ndt.iam.ntu.edu.tw)

The authors are with the Institute of Applied Mechanics, National Taiwan University, Taipei, Taiwan 106, R.O.C.

ter on diamond. Recently, Wu and Chen (2002) calculated exactly the velocity dispersion and the electromechanical coefficients of a ZnO/Diamond/Si layered medium with an interdigital transducer (IDT) on the surface by using the effective permittivity approach. In their paper, the mismatch induced by using Ingebrigtsen's approximation to calculate the electromechanical coefficient was reported.

In this paper, we utilized the effective permittivity approach to calculate the electromechanical coupling coefficients of surface acoustic waves in layered systems. The formulation based on the matrix method (Stroh, 1962; Fahmy and Adler, 1973; Ingebrigtsen and Tonning, 1969; Honein *et al*., 1991) for calculating the effective permittivity of a layered piezoelectric medium with three types of electrode arrangements is given. Based on this formulation, we calculated phase velocity dispersions and the electromechanical coupling coefficients of surface acoustic waves in layered systems of ZnO/Diamond and $LiNbO_3$/Diamond. In the calculations, three different types of electrical boundary conditions were analyzed and discussed.

II. FORMULATION

1. Effective Permittivity of a Layered Piezoelectric Medium

In the quasi-static approximation, the governing field equations of piezoelectricity can be express as

$$\sigma_{ij,\,j}=\rho\ddot{u}_i, \tag{1}$$

$$D_{i,\,i}=0 \tag{2}$$

where ρ is the mass density and D_i is the electric displacement. σ_{ij} and u_i are the Cauchy stress tensor and mechanical displacement, respectively. The piezoelectric constitutive relations with the displacement u_i and electric potential ϕ as variables are of the form

$$\sigma_{ij}=C_{ijkl}u_{k,\,l}+e_{lij}\phi_{,\,l} \tag{3}$$

$$D_i=e_{ikl}u_{k,\,l}-\varepsilon_{il}\phi_{,\,l} \tag{4}$$

In these equations, C_{ijkl} is the elastic stiffness at constant electric field of the piezoelectric medium, e_{lij} is the piezoelectric constants, and ε_{il} is the dielectric constants at constant strain. For plane harmonic wave propagating in the x-direction, the displacement vector $\boldsymbol{u}$, the z-component of the electric displacement vector D_z, the traction vector $\boldsymbol{t}$, and the electric potential ϕ are given by

$$\boldsymbol{u}(x,\,y,\,z)=\overline{\boldsymbol{u}}\,(z)\exp\{i(\omega t-k_x x)\} \tag{5}$$

$$D_z(x,\,y,\,z)=\overline{D}_z(z)\exp\{i(\omega t-k_x x)\} \tag{6}$$

$$\boldsymbol{t}(x,\,y,\,z)=\overline{\boldsymbol{t}}\,(z)\exp\{i(\omega t-k_x x)\} \tag{7}$$

$$\phi(x,\,y,\,z)=\overline{\phi}\,(z)\exp\{i(\omega t-k_x x)\} \tag{8}$$

where ω is the circular frequency and k_x is the x-component wave vector of the plane harmonic waves. According to the state vector formulation of elastic waves in anisotropic solids, the governing Eqs. (1)-(4) can be arranged in the matrix form as (Stroh, 1962; Fahmy and Adler, 1973; Ingebrigtsen and Tonning, 1969; Honein *et al*., 1991) :

$$\frac{d}{dz}\overline{\xi}\,(z)=-i\boldsymbol{N}(z)\overline{\xi}\,(z)\,,\ \text{with}\ \overline{\xi}\,(z)=\begin{Bmatrix}\overline{\boldsymbol{u}}\,(z)\\ \overline{\phi}\,(z)\\ i\overline{\boldsymbol{t}}\,(z)\\ i\overline{D}_z(z)\end{Bmatrix} \tag{9}$$

where $\overline{\xi}\,(z)$ is the state vector and $\boldsymbol{N}(z)$ is called the fundamental acoustic tensor. The solution of this system of differential equations can be expressed as

$$\overline{\xi}\,(z)=e^{-i\boldsymbol{N}(z)}\overline{\xi}\,(0) \tag{10}$$

where $e^{-iN(z)}$ is called the transfer matrix and the initial condition at z=0 is $\overline{\xi}\,(0)$. This solution is appropriate for a layered system, because the overall solution can be obtained by multiplication of the solutions of each layer. For multilayered media, the surface impedance approach can be adopted to avoid the numerical difficulties (Ingebrigtsen and Tonning, 1969; Honein *et al*., 1991). Using this approach, the generalized traction vector $\boldsymbol{T}=\{i\overline{\boldsymbol{t}}\,(z)\ i\overline{D}_z(z)\}^T$ and the generalized displacement vector $\boldsymbol{U}=\{\overline{\boldsymbol{u}}\,(z)\ \overline{\phi}\,(z)\}^T$ are defined at a plane normal to the z-axis. On using the eigenvalue-eigenvector decomposition of the transfer matrix, Eq. (10) can be arranged in the form

$$\begin{Bmatrix}\boldsymbol{U}\\ \boldsymbol{T}\end{Bmatrix}=\begin{bmatrix}\boldsymbol{A}_1 & \boldsymbol{A}_2\\ \boldsymbol{L}_1 & \boldsymbol{L}_2\end{bmatrix}\begin{bmatrix}\boldsymbol{\Phi}_1 & \boldsymbol{0}\\ \boldsymbol{0} & \boldsymbol{\Phi}_2\end{bmatrix}\begin{Bmatrix}\boldsymbol{C}_1\\ \boldsymbol{C}_2\end{Bmatrix} \tag{11}$$

where $\begin{bmatrix}\boldsymbol{A}_1 & \boldsymbol{A}_2\\ \boldsymbol{L}_1 & \boldsymbol{L}_2\end{bmatrix}$ is the matrix of eigenvalues of $\boldsymbol{N}$, which are arranged such that the first four eigenvalues of $\boldsymbol{N}$ correspond to waves decaying in the z-direction, and $\boldsymbol{A}_1$, $\boldsymbol{A}_2$, $\boldsymbol{L}_1$, $\boldsymbol{L}_2$ are 4×4 matrices. $\boldsymbol{C}_1$, $\boldsymbol{C}_2$ are constant vectors and are related to the initial condition at z=0. The diagonal matrices are

$$\boldsymbol{\Phi}_1=\mathrm{diag}(e^{-ik_{z1}z},\ e^{-ik_{z2}z},\ e^{-ik_{z3}z},\ e^{-ik_{z3}z})$$

$$\boldsymbol{\Phi}_2=\mathrm{diag}(e^{-ik_{z5}z}, e^{-ik_{z6}z}, e^{-ik_{z7}z}, e^{-ik_{z8}z}) \tag{12}$$

with k_{zi} the eigenvalues of $\boldsymbol{N}$. With the above arrangement of the transfer matrix, the surface impedance tensor of the layered piezoelectric medium can be defined as (Honein *et al*., 1991)

$$\boldsymbol{T}=i\omega\boldsymbol{G}\boldsymbol{U} \tag{13}$$

where the surface impedance tensor $\boldsymbol{G}$ is a 4×4 matrix. The recursive formulas of $\boldsymbol{G}$ for layered media are then given by

$$\boldsymbol{G}_j=[\boldsymbol{Z}_{1j}\boldsymbol{W}_{1j}(z)\boldsymbol{R}_{j-1}\boldsymbol{W}_{2j}^{-1}+\boldsymbol{Z}_{2j}][\boldsymbol{W}_{1j}(z)\boldsymbol{R}_{j-1}\boldsymbol{W}_{2j}^{-1}+\boldsymbol{I}]^{-1} \tag{14}$$

$$\boldsymbol{Z}_{\alpha j}=-\frac{1}{\omega}\boldsymbol{L}_{\alpha j}\boldsymbol{A}_{\alpha j}^{-1}{}_{\alpha j} \tag{15}$$

$$\boldsymbol{W}_{\alpha j}=\boldsymbol{A}_{\alpha j}\boldsymbol{\Phi}_{\alpha j}\boldsymbol{A}_{\alpha j}^{-1} \tag{16}$$

$$\boldsymbol{R}_{j-1}=[\boldsymbol{Z}_{1j}-\boldsymbol{G}_{j-1}]^{-1}[\boldsymbol{G}_{j-1}-\boldsymbol{Z}_{2j}] \tag{17}$$

where $\boldsymbol{Z}_{\alpha j}$ are local impedances for the up-going wave and the down-going wave. α=1 represents decaying waves in the positive z-direction (up-going), and α=2 represents decaying waves in the negative z-direction (down-going).

For convenience in defining the effective permittivity, the surface impedance tensor $\boldsymbol{G}$ can be arranged in the form

$$\boldsymbol{G}=\begin{bmatrix}\boldsymbol{G}_m & \boldsymbol{g}_{T\phi}\\ \boldsymbol{g}_{DU}^T & g_{D\phi}\end{bmatrix} \tag{18}$$

where the 3×3 matrix $\boldsymbol{G}_m$ is the mechanical part of $\boldsymbol{G}$. The 3×1 vectors $\boldsymbol{g}_{T\phi}$ and $\boldsymbol{g}_{DU}^T$ are the electromechanical coupling terms of $\boldsymbol{G}$. $\boldsymbol{g}_{T\phi}$ is the coupling between the traction and the electric potential, and $\boldsymbol{g}_{DU}$ is the coupling between electric displacement and particle displacement. $\boldsymbol{g}_{D\phi}$ is a scalar which relates the electric potential to the electric displacement. The superscript "T" in $\boldsymbol{g}_{DU}^T$ denotes the transpose. The scalar $\boldsymbol{g}_{D\phi}$ relates the electric potential to the electric displacement. Eq. (13) can be expanded as

$$i\overline{\boldsymbol{t}}=i\omega[\boldsymbol{G}_m\overline{\boldsymbol{u}}+\boldsymbol{g}_{T\phi}\overline{\phi}] \tag{19}$$

$$i\overline{D}_z=i\omega[\boldsymbol{g}_{DU}^T\overline{\boldsymbol{u}}+\boldsymbol{g}_{D\phi}\overline{\phi}] \tag{20}$$

In the following derivation, we consider three different types of electrode arrangements of a layered half-space structure in contact with a vacuum as shown in Fig. 1. The first one (type A) is a layered half-space structure with IDTs deposited on the top surface and free interface. The second one (type B) has IDTs arranged in the interface between the layer and the half-space and its top surface is open-circuited (free). In the third one (type C), the IDTs are also arranged in the interface between the layer and the half-space and the top surface is short-circuited (metallized).

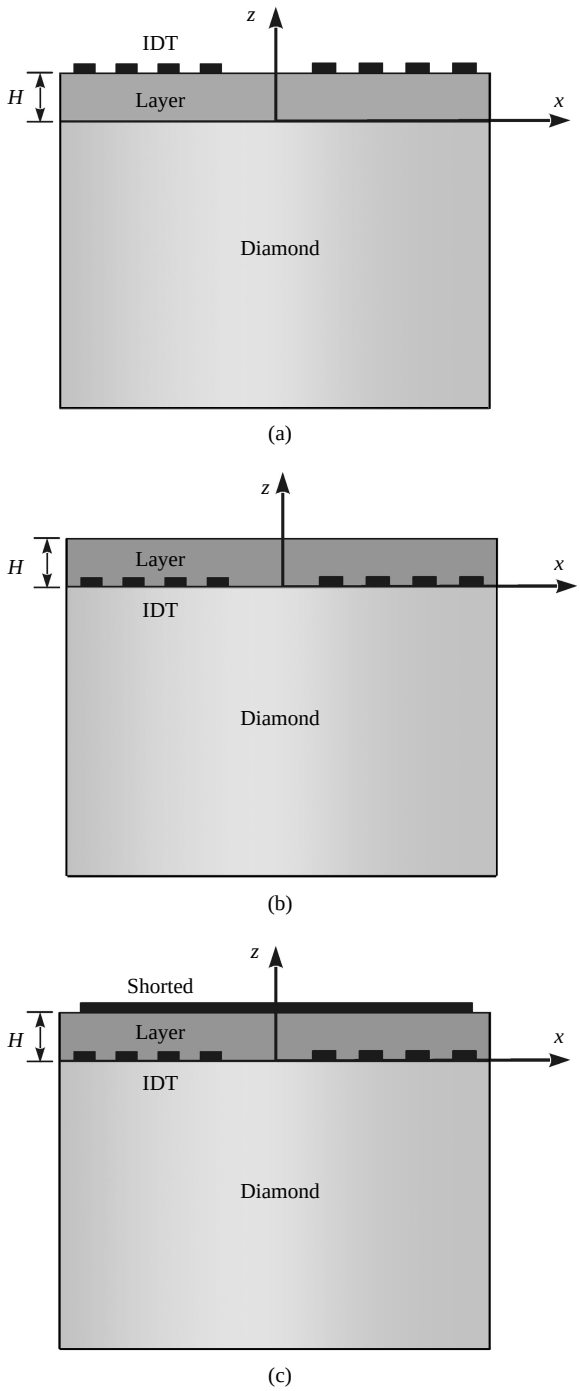

Fig. 1 Coordinates of the layered half space. (a) type A; (b) type B; (c) type C.

In the layered structure of type A, the tractions on the top surface are vanishing. The electric displacement at $z=H$ in the solid side is denoted as

$\overline{D}_z\big|_{z=H^-}$ (Fig. 1) and is given by

$$\overline{D}_z\big|_{z=H^-} = \omega(-\boldsymbol{g}_{DU}^T\boldsymbol{G}_m^{-1}\boldsymbol{g}_{T\phi} + \boldsymbol{g}_{D\phi})\,\overline{\phi}\,\big|_{z=H^-} \quad (21)$$

In the vacuum, $z>H$, the electric potential satisfies the Laplace equation. The normal electric displacement $\overline{D}_z\big|_{z=H^+}$ at $z=H$ in the vacuum side is given by $\overline{D}_z\big|_{z=H^+} = \varepsilon_0 k_x\,\overline{\phi}\,\big|_{z=H^+}$. The effective permittivity at the interface between the vacuum and the layer can then be written as

$$\varepsilon_s = \frac{\overline{D}_z\big|_{z=H^+} - \overline{D}_z\big|_{z=H^-}}{k_x\,\overline{\phi}\,\big|_{z=H}} = \varepsilon_0 - \frac{\omega}{k_x}(-\boldsymbol{g}_{DU}^T\boldsymbol{G}_m^{-1}\boldsymbol{g}_{T\phi} + \boldsymbol{g}_{D\phi}) \quad (22)$$

where the continuity of the electric potential at the interface has been employed.

For the case of type B, to satisfy the boundary conditions of the top surface at $z=H$, which include traction free and the continuity of the normal electric displacement, the surface impedance tensor $\boldsymbol{G}$ of the top surface can be expressed as

$$\boldsymbol{G}\big|_{z=H} = \begin{bmatrix} \mathbf{0} & \mathbf{0} \\ \mathbf{0} & -i\varepsilon_0 k_x \end{bmatrix} \quad (23)$$

where the Laplace equation of the electric potential in the vacuum has been satisfied.

At the interface between the layer and half-space, the relation between the generalized traction vector and displacement vector at $z=0^+$ in the layer side can be expressed as

$$\left.\begin{Bmatrix} i\overline{\boldsymbol{t}} \\ i\overline{D}_z \end{Bmatrix}\right|_{z=0^+} = i\omega\boldsymbol{G}\left.\begin{Bmatrix} \overline{\boldsymbol{u}} \\ \overline{\phi} \end{Bmatrix}\right|_{z=0^+} = i\omega\begin{bmatrix} \boldsymbol{G}_m^+ & \boldsymbol{g}_{T\phi}^+ \\ \boldsymbol{g}_{DU}^{T+} & g_{D\phi}^+ \end{bmatrix}\left.\begin{Bmatrix} \overline{\boldsymbol{u}} \\ \overline{\phi} \end{Bmatrix}\right|_{z=0^+} \quad (24)$$

and at $z=0^-$ in the diamond substrate side, we have

$$\left.\begin{Bmatrix} i\overline{\boldsymbol{t}} \\ i\overline{D}_z \end{Bmatrix}\right|_{z=0^-} = i\omega\boldsymbol{G}^-\left.\begin{Bmatrix} \overline{\boldsymbol{u}} \\ \overline{\phi} \end{Bmatrix}\right|_{z=0^-} = i\omega\begin{bmatrix} \boldsymbol{G}_m^- & \boldsymbol{g}_{T\phi}^- \\ \boldsymbol{g}_{DU}^{T-} & g_{D\phi}^- \end{bmatrix}\left.\begin{Bmatrix} \overline{\boldsymbol{u}} \\ \overline{\phi} \end{Bmatrix}\right|_{z=0^-} \quad (25)$$

Since the traction, mechanical displacement and electric potential at the interface $z=0$ are continuous, the z-component of the electric displacements on both sides of the interface are therefore given by

$$\overline{D}_z\big|_{z=0^+} = \omega[\boldsymbol{g}_{DU}^{T+}(\boldsymbol{G}_m^- - \boldsymbol{G}_m^+)^{-1}(\boldsymbol{g}_{T\phi}^+ - \boldsymbol{g}_{T\phi}^-) + g_{D\phi}^+]\,\overline{\phi}\,\big|_{z=0} \quad (26)$$

$$\overline{D}_z\big|_{z=0^-} = \omega[\boldsymbol{g}_{DU}^{T-}(\boldsymbol{G}_m^- - \boldsymbol{G}_m^+)^{-1}(\boldsymbol{g}_{T\phi}^+ - \boldsymbol{g}_{T\phi}^-) + g_{D\phi}^-]\,\overline{\phi}\,\big|_{z=0} \quad (27)$$

Accordingly, the effective permittivity at the interface between the layer and diamond substrate can be written as

$$\varepsilon_s = \frac{\overline{D}_z\big|_{z=0^+} - \overline{D}_z\big|_{z=0^-}}{k_s\,\overline{\phi}\,\big|_{z=0}} = \frac{\omega}{k_x}[(\boldsymbol{g}_{DU}^{T+} - \boldsymbol{g}_{DU}^{T-})(\boldsymbol{G}_m^- - \boldsymbol{G}_m^+)^{-1}(\boldsymbol{g}_{T\phi}^+ - \boldsymbol{g}_{T\phi}^-) + g_{D\phi}^+ - g_{D\phi}^-] \quad (28)$$

For the case of type C, to satisfy the boundary conditions of the top surface at $z=H$, the surface impedance tensor $\boldsymbol{G}$ of the top surface can be expressed as

$$\boldsymbol{G}\big|_{z=H} = \mathbf{0} \quad (29)$$

At the interface between the layer and a diamond substrate, the relation between the generalized traction vector and displacement vector at $z=0^+$ in the layer side can be expressed as

$$\left.\begin{Bmatrix} i\overline{\boldsymbol{t}} \\ \overline{\phi} \end{Bmatrix}\right|_{z=0^+} = i\omega\boldsymbol{G}^+\left.\begin{Bmatrix} \overline{\boldsymbol{u}} \\ i\overline{D}_z \end{Bmatrix}\right|_{z=0^+} = i\omega\begin{bmatrix} \boldsymbol{G}_m^+ & \boldsymbol{g}_{TD}^+ \\ \boldsymbol{g}_{\phi U}^{T+} & g_{\phi D}^+ \end{bmatrix}\left.\begin{Bmatrix} \overline{\boldsymbol{u}} \\ i\overline{D}_z \end{Bmatrix}\right|_{z=0^+} \quad (30)$$

and at $z=0^-$ in the diamond substrate side, we have

$$\left.\begin{Bmatrix} i\overline{\boldsymbol{t}} \\ \overline{\phi} \end{Bmatrix}\right|_{z=0^-} = i\omega\boldsymbol{G}^-\left.\begin{Bmatrix} \overline{\boldsymbol{u}} \\ i\overline{D}_z \end{Bmatrix}\right|_{z=0^-} = i\omega\begin{bmatrix} \boldsymbol{G}_m^- & \boldsymbol{g}_{TD}^- \\ \boldsymbol{g}_{\phi U}^{T-} & g_{\phi D}^- \end{bmatrix}\left.\begin{Bmatrix} \overline{\boldsymbol{u}} \\ i\overline{D}_z \end{Bmatrix}\right|_{z=0^-} \quad (31)$$

Since the traction, mechanical displacement and electric potential are continuous at the interface, the z-component of the electric displacements on both sides of the interface are expressed as

$$i\overline{D}_z\big|_{z=0^+} = \{ -\frac{\boldsymbol{g}_{\phi U}^{T+}}{g_{\phi D}^{+}}[i\omega(\boldsymbol{G}_m^{-} - \frac{\boldsymbol{g}_{TD}^{-}\boldsymbol{g}_{\phi U}^{T-}}{g_{\phi D}^{-}}) - i\omega(\boldsymbol{G}_m^{+} - \frac{\boldsymbol{g}_{TD}^{+}\boldsymbol{g}_{\phi U}^{T+}}{g_{\phi D}^{+}})]^{-1}[\frac{\boldsymbol{g}_{TD}^{+}}{g_{\phi D}^{+}} - \frac{\boldsymbol{g}_{TD}^{-}}{g_{\phi D}^{-}}] + \frac{1}{g_{\phi D}^{+}}\}\,\overline{\phi}\,\big|_{z=0} \tag{32}$$

$$i\overline{D}_z\big|_{z=0^-} = \{ -\frac{\boldsymbol{g}_{\phi U}^{T-}}{g_{\phi D}^{-}}[i\omega(\boldsymbol{G}_m^{-} - \frac{\boldsymbol{g}_{TD}^{-}\boldsymbol{g}_{\phi U}^{T-}}{g_{\phi D}^{-}} - i\omega(\boldsymbol{G}_m^{+} - \frac{\boldsymbol{g}_{TD}^{+}\boldsymbol{g}_{\phi U}^{T+}}{g_{\phi D}^{+}})]^{-1}[\frac{\boldsymbol{g}_{TD}^{+}}{g_{\phi D}^{+}} - \frac{\boldsymbol{g}_{TD}^{-}}{g_{\phi D}^{-}}] + \frac{1}{g_{\phi D}^{-}}\}\,\overline{\phi}\,\big|_{z=0} \tag{33}$$

The effective permittivity at the interface can then be written as

$$\varepsilon_s = \frac{\overline{D}_z\big|_{z=0^+} - \overline{D}_z\big|_{z=0^-}}{k_s\,\overline{\phi}\,\big|_{z=0}}$$

$$= \frac{1}{ik_x}\{\{ -\frac{\boldsymbol{g}_{\phi U}^{T+}}{g_{\phi D}^{+}}[i\omega(\boldsymbol{G}_m^{-} - \frac{\boldsymbol{g}_{TD}^{-}\boldsymbol{g}_{\phi U}^{T-}}{g_{\phi D}^{-}}) - i\omega(\boldsymbol{G}_m^{+} - \frac{\boldsymbol{g}_{TD}^{+}\boldsymbol{g}_{\phi U}^{T+}}{g_{\phi D}^{+}})]^{-1}[\frac{\boldsymbol{g}_{TD}^{+}}{g_{\phi D}^{+}} - \frac{\boldsymbol{g}_{TD}^{-}}{g_{\phi D}^{-}}] + \frac{1}{g_{\phi D}^{+}}\}$$

$$- \{ -\frac{\boldsymbol{g}_{\phi U}^{T-}}{g_{\phi D}^{-}}[i\omega(\boldsymbol{G}_m^{-} - \frac{\boldsymbol{g}_{TD}^{-}\boldsymbol{g}_{\phi U}^{T-}}{g_{\phi D}^{-}}) - i\omega(\boldsymbol{G}_m^{+} - \frac{\boldsymbol{g}_{TD}^{+}\boldsymbol{g}_{\phi U}^{T+}}{g_{\phi D}^{+}})]^{-1}[\frac{\boldsymbol{g}_{TD}^{+}}{g_{\phi D}^{+}} - \frac{\boldsymbol{g}_{TD}^{-}}{g_{\phi D}^{-}}] + \frac{1}{g_{\phi D}^{-}}\}\} \tag{34}$$

2. Electromechanical Coupling Coefficient

The electromechanical coupling coefficient K_s^2 can be defined in terms of the effective permittivity as (Matthews, 1997)

$$K_s^2 = 2\Gamma_s\varepsilon_s^{(\infty)} \tag{35}$$

where $\varepsilon_s^{(\infty)}$ is the effective permittivity at infinite slowness. The function Γ_s is defined as (Morgan, 1991)

Table 1 The material constants used in the calculation (Nakahata *et al.*, 1995)

		Diamond	ZnO	$LiNbO_3$
Elastic constants (10^{11} N/m^2)	C_{11}	10.8	2.10	2.03
	C_{12}		1.211	0.53
	C_{13}	1.25	1.05	0.752
	C_{33}	10.8	2.11	2.424
	C_{44}	5.76	0.423	0.595
Piezoelectric constants (C/m^2)	e_{15}		-0.480	3.76
	e_{31}		-0.573	0.23
	e_{33}		1.321	1.33
Relative dielectric constants	ε_{11}	5.70	8.55	44.3
	ε_{33}	5.70	10.2	27.9
Mass density (10^3 kg/m^3)	ρ	3.51	5.67	4.64

$$\frac{1}{\Gamma_s} = -\beta[\frac{d\varepsilon_s(k_s)}{dk_x}]_\beta \tag{36}$$

The wave number $\beta(\omega)$ is taken to be $\beta(\omega)=\frac{\omega}{v_0(\omega)}$, where v_0 is the surface wave velocity under open-circuited interface condition which can be obtained from the dispersion relation. On the other hand, by using the Ingebrigtsen approximation (Ingebrigtsen, 1969), the electromechanical coupling coefficient of a piezoelectric medium can be approximated as

$$K_s^2 = 2\,\frac{v_0 - v_m}{v_0} \tag{37}$$

where v_m is the surface wave velocity under short-circuited condition.

III. RESULTS AND DISCUSSION

In the following, a detailed calculation was made on ZnO/diamond and $LiNbO_3$/diamond layered structures. Based on the aforementioned formulation, effective permittivity, phase velocity and the electromechanical coupling coefficient of the structures with three different types of electrical boundary conditions were calculated and discussed. The relative material constants used in the calculations are listed in Table 1. In the calculations, the $LiNbO_3$ film was treated as a class 6mm material, and their C_{14} and e_{22} were set equal to zero (Nakahata *et al.*, 1995).

1. ZnO/Diamond Layered Half-Space

First, we considered an infinite half-space diamond substrate with an overlay of ZnO. Both materials have their crystalline Z-axis normal to the

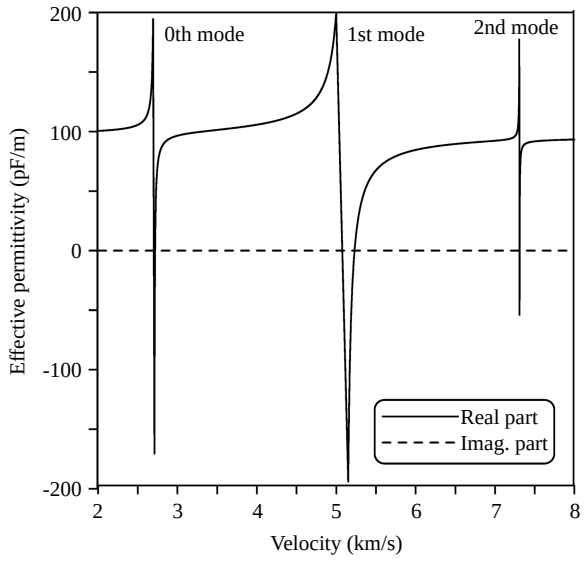

Fig. 2 Plot of the effective permittivity of a ZnO/Diamond layered half space for electrode arrangement of Type A as a function of the phase velocity. (*fH*=3000MHz)

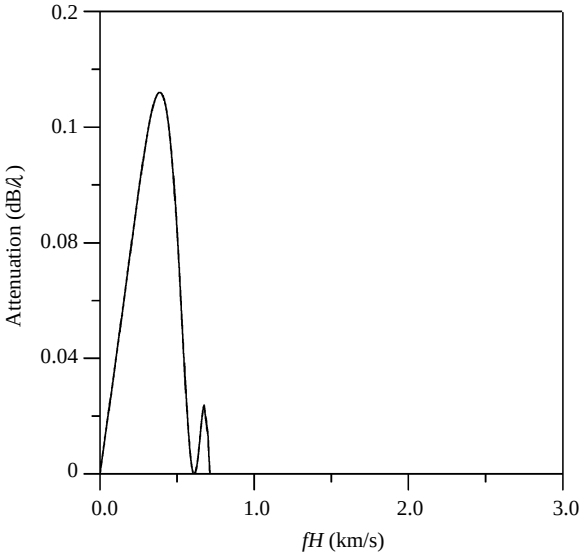

Fig. 4 Wave attenuation of the HVPSAW mode in the ZnO/Diamond structure for type A as a function of *fH*.

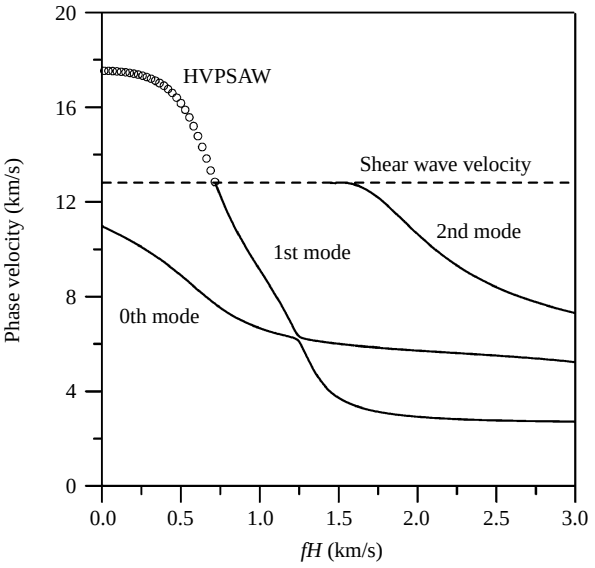

Fig. 3 Phase velocity dispersion of the first three SAW modes in the ZnO/Diamond structure for type A as a function of *fH*.

interface and the propagation (*x*-axis) is chosen along the crystalline *X*-axis. Shown in Fig. 2 is the plot of the effective permittivity as a function of phase velocity for electrode arrangement of type A at frequency-thickness *fH*=3 km/s. In the figure, the solid line represents the real part of the effective permittivity, and the dashed line represents the imaginary part. The effective permittivity is real in this case, which indicates that there is no acoustic energy leaked into the substrate. The plot shows that there exist a pole and a zero for phase velocities around 2718 m/s (the oth mode). Similar pole and zero are found for phase velocity close to 5231 m/s (the first mode), as well as 7310 m/s (the second mode). The zeros correspond to the surface wave solution for a free surface, since the charge density is zero. The poles indicate the surface wave solution for a metallized surface, since it gives a finite charge density at zero electric potential.

Shown in Fig. 3 are the phase velocity dispersion relations of the first three SAW modes in the ZnO/diamond layered structure for the electrode arrangement of type A. The dispersion was calculated based on the aforementioned effective permittivity approach. The results show that every mode has a much higher velocity than the conventional materials. The velocities show dispersion characteristics and are decreased with increasing *fH*. For the second mode SAW, the cutoff velocity exists which occurs at the shear bulk wave velocity of diamond, i.e., about 12.810 km/s. It is worth noting that the dispersion curves of the first two SAW modes are very close to each other in some regions, but do not cross. At frequency-thickness *fH*=1247 m/s, there exists a high curvature bend for both of the first two modes. Instead of decreasing smoothly, the first mode of surface acoustic wave bends down at *fH*=1247 m/s and the second mode bends up. As will be shown later, the frequency at which the phase velocity changes sharply corresponds to a sharp change in the electromechanical coupling coefficient for both modes.

For velocity higher than the shear bulk wave velocity of diamond, the second generalized SAW mode becomes pseudo SAW. In the pseudo SAW mode, a small part of the energy leaks into the

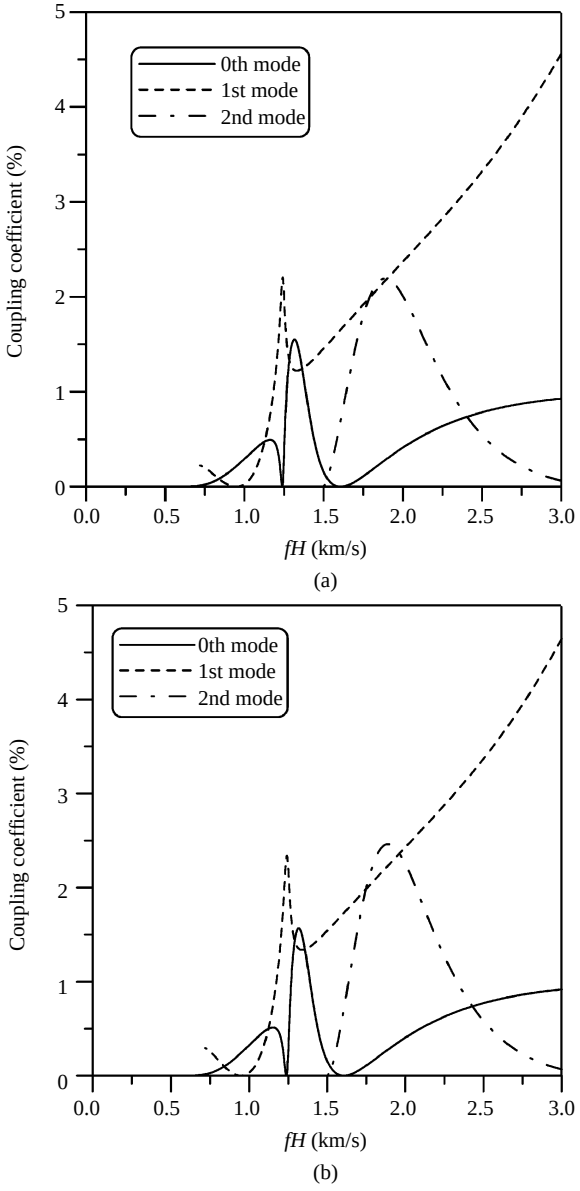

Fig. 5 Electromechanical coupling coefficients of the ZnO/Diamond structure for type A calculated by using (a) Ingebrigtsen's approximation and (b) the effective permittivity.

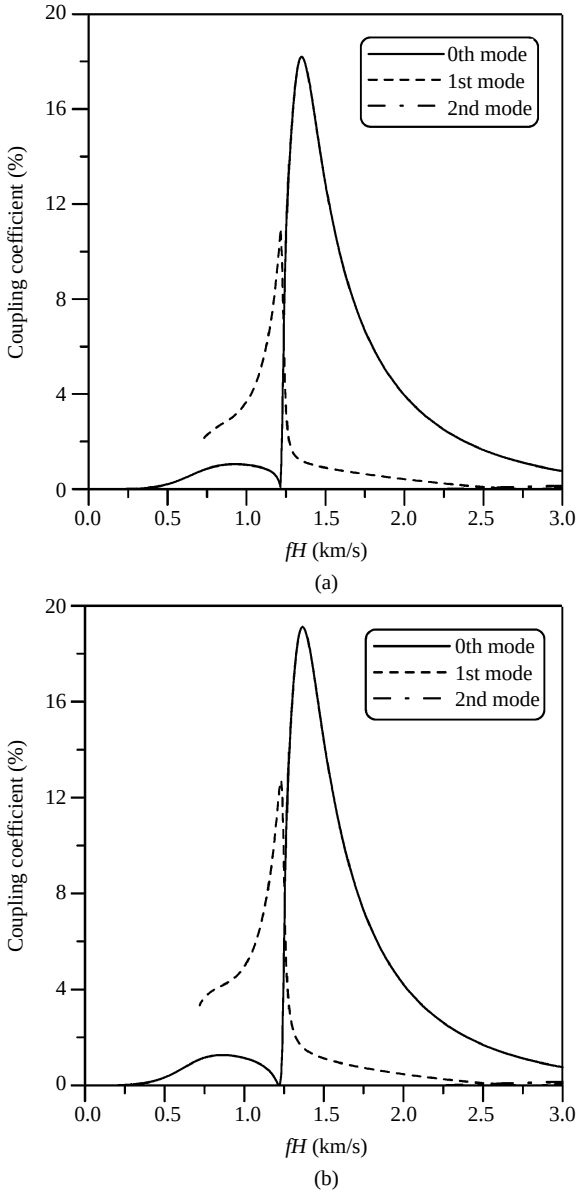

Fig. 6 Electromechanical coupling coefficients of the ZnO/Diamond structure for type B calculated by using (a) Ingebrigtsen's approximation and (b) the effective permittivity.

layered half space and leads to propagation losses. In Fig. 2, the high velocity pseudo surface acoustic wave (HVPSAW) mode is shown by circles. It extends from the shear bulk wave velocity of diamond to 17.542 km/s, which is the longitudinal bulk wave of diamond. Shown in Fig. 3 is the plot of the propagation loss of the HVPSAW mode. It's worth noting that at *fH* of 0.61 km/s, the minimum value of the propagation loss is about 1.8×10^{-6} dB/λ and its velocity is equal to 14.747 km/s. Because this loss doesn't cause problems in practice, the HVPSAW mode in ZnO/diamond structure can be used to design an ultrahigh frequency SAW device due to its high velocity.

In this section, we calculated the electromechanical coupling coefficients of the ZnO/diamond layered structure for three types of electrode arrangements based on the effective permittivity and the Ingebrigtsen approximation. The calculated results are shown in Fig. 5, 6 and 7, which are for electrode arrangements of type A, type B and type C, respectively. In these three figures, (a) and (b) represent the results calculated based on the Ingebrigtsen approximation and the effective permittivity, respectively. The plots show that, by applying the constant frequency as the independent variable, the calculated results from the

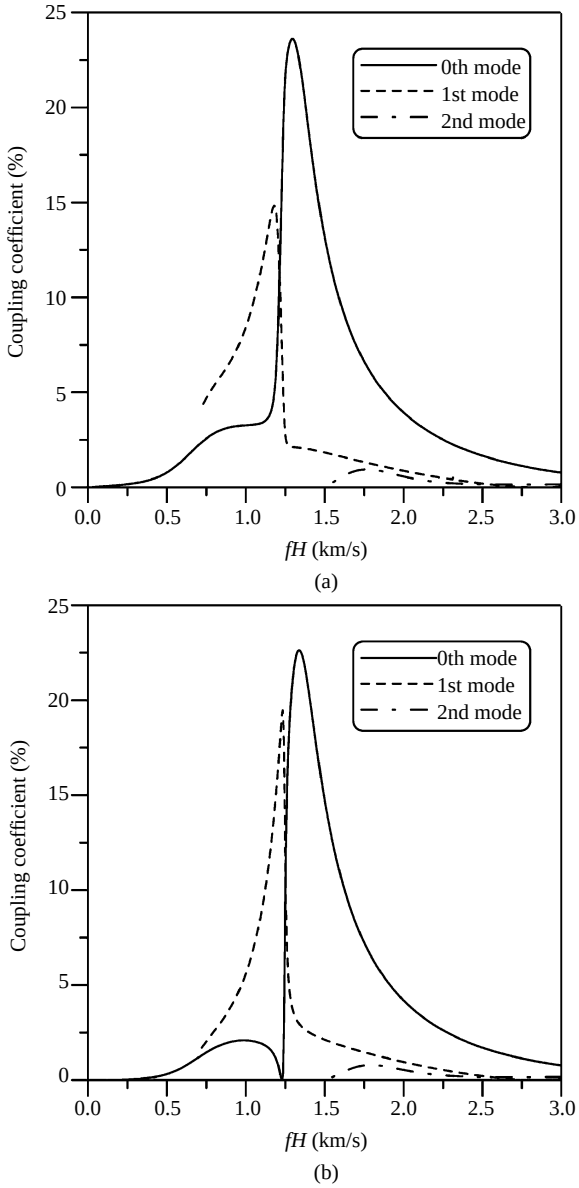

Fig. 7 Electromechanical coupling coefficients of the ZnO/Diamond structure for type C calculated by using (a) Ingebrigtsen's approximation and (b) the effective permittivity.

effective permittivity are close to those calculated based on the Ingebrigtsen approximation. This was also mentioned in the literature (Adler and Solie, 1995; Wu and Chen, 2002). In addition, we found that the frequency at which the phase velocity of the 0th and 1st mode changes sharply corresponds to sharp changes in the electromechanical coupling coefficients for both modes. At the sharp change frequency, K_s^2 values of the zeroth mode go to almost zero and are maximized for the first mode.

The results in Figs. 5(b), 6(b) and 7(b) also show that the electromechanical coupling coefficients are sensitive to the electrical boundary conditions. For

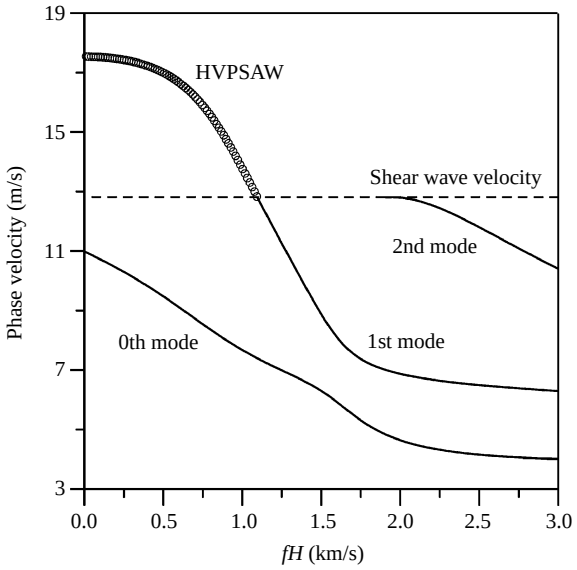

Fig. 8 Phase velocity dispersion of the first three SAW modes in the $LiNbO_3$/Diamond structure for type A as a function of *fH*.

the zeroth mode, the electromechanical coupling coefficients have maximum values of about 1.6% for type A, 19.1% for type B and 22.6% for type C in the frequency-thickness range smaller than 3 km/s, respectively. For the first mode, the electromechanical coupling coefficients have maximum values of about 4.6% for type A, 12.7% for type B and 19.4% for type C, respectively. The maximum of the electromechanical coupling coefficients of the second mode are all smaller than 3% regardless of the electrode arrangement. Accordingly, we conclude that to obtain a large electromechanical coupling coefficient, the ZnO/diamond structure, with IDTs located at the interface between the ZnO layer and a diamond substrate, is preferred.

2. $LiNbO_3$/Diamond Layered Half-Space

$LiNbO_3$ is a well-known single-crystal piezoelectric material and is being used widely as a substrate material for SAW devices due to its high electromechanical coupling coefficient. Recently, the c-axis oriented $LiNbO_3$ film deposited on a diamond substrate has been studied (Nakahata *et al.*, 1995). In the following, the phase velocity and electromechanical coupling coefficient of a diamond substrate with an overlay of the *c*-axis oriented $LiNbO_3$ film are analyzed based on the aforementioned effective permittivity approach. Both materials have their crystalline *Z*-axis normal to the interface and the propagation (*x*-axis) is chosen along the crystalline *X*-axis. Shown in Fig. 8 is the plot of the calculated phase velocity dispersions of the first three SAW modes in

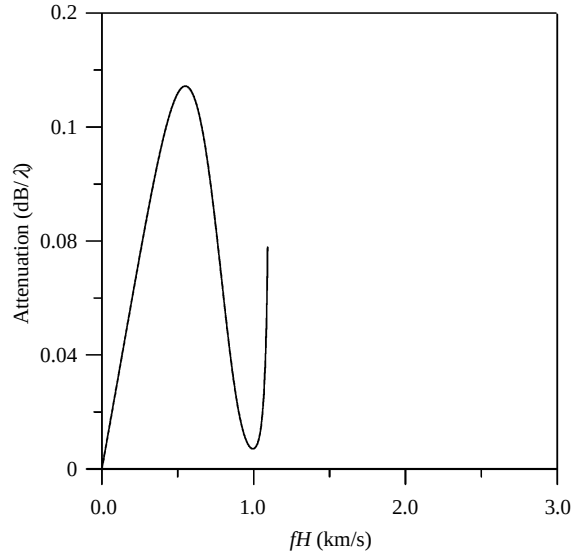

Fig. 9 Wave attenuation of the HVPSAW mode in the $LiNbO_3$/Diamond structure for type A as a function of *fH*.

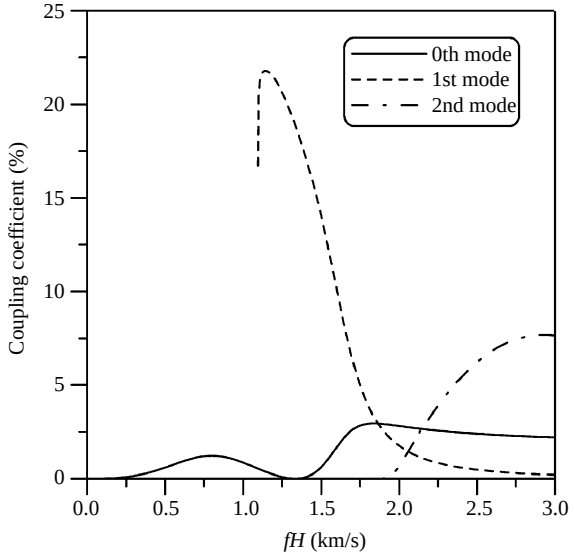

Fig. 10 Electromechanical coupling coefficients of the $LiNbO_3$/Diamond structure for type A calculated by using the effective permittivity.

the $LiNbO_3$/diamond layered structure for the electrode arrangement of type A. The results show that the velocities are larger than those of ZnO/diamond. This is because ZnO has a smaller velocity than $LiNbO_3$. These velocities also show dispersion characteristics and are decreased with increasing *fH*. For the 2nd mode SAW, the cutoff velocity exists and is about 12.810 km/s, which is the shear bulk wave velocity of diamond. In addition, for velocity higher than the shear bulk wave velocity of diamond, the second generalized SAW mode becomes pseudo SAW. In the pseudo SAW mode, a small part of the energy leaks into the layered half space and leads to some propagation losses. In Fig. 8, the HVPSAW mode is shown by circles. It extends from the shear bulk wave velocity of diamond to the longitudinal bulk wave velocity. The calculated propagation loss of the HVPSAW mode as a function of *fH* is shown in Fig. 9. We note that at *fH* of 1 km/s, the minimum value of the propagation loss is about 7.1×10^{-3} dB/λ, which is higher than in the ZnO/diamond layered structure. This loss may cause problems in practical RF SAW filters.

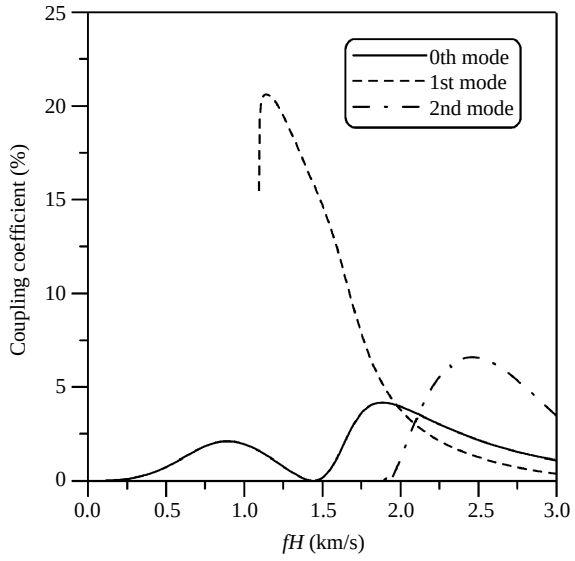

Fig. 11 Electromechanical coupling coefficients of the $LiNbO_3$/Diamond structure for type B calculated by using the effective permittivity.

The electromechanical coupling coefficients calculated based on the effective permittivity are shown in Fig. 10, 11 and 12, which are for electrode arrangements of type A, type B amd type C, respectively. In these three figures, the solid line, the dashed line and the dot-dashed line represent the electromechanical coupling coefficients of the zeroth, first and second mode, respectively. The results show that, for type A and type B, the electromechanical coupling coefficient of the first mode is larger than the other two modes. It reaches the maximum of 21. 8% km/s for type A and 20.6% for type B, and both the maximums happen at *fH*=1.14. It is worth noting that the electromechanical coupling coefficient of the second mode for type C has a large velocity of 12.26 km/s and large K_s^2 18.4% at *fH*=2.33 km/s. These two findings are useful for the design of a SAW device based on the $LiNbO_3$/diamond layered structure.

IV. CONCLUSION

A study of the electromechanical coupling

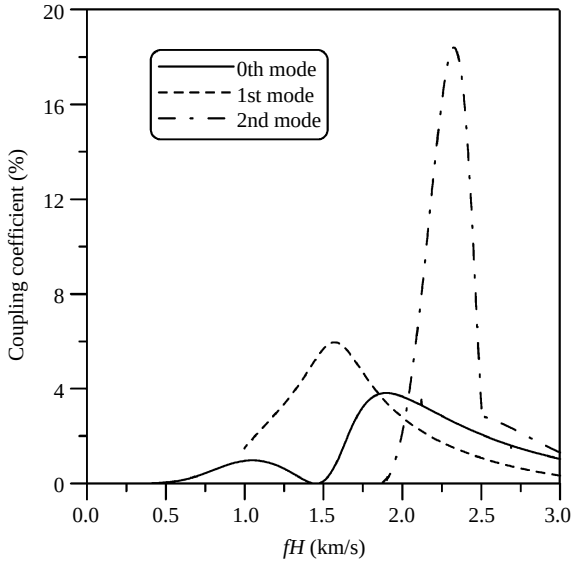

Fig. 12 Electromechanical coupling coefficients of the $LiNbO_3$/Diamond structure for type C calculated by using the effective permittivity.

coefficients of surface acoustic waves in layered systems based on the effective permittivity approach is presented. The formulation based on the matrix method for calculating the effective permittivity of a layered piezoelectric medium is given, and used to calculate the phase velocity dispersion and the electromechanical coupling coefficient of the layered system. In our calculations, three different types of electrode arrangements were considered. The results of wave attenuation of the HVPSAW mode provide a guide rule to select a proper wave frequency or layer thickness. In the calculation of the electromechanical coefficient of the ZnO/diamond structure, results show that the sharp change of phase velocity in the dispersion curve is intimately related to the sharp change of the electromechanical coupling coefficient. Finally, according to our calculated results, we suggest that the second SAW mode of the $LiNbO_3$/diamond for type *C* is a good choice for an ultrahigh frequency SAW device due to its high velocity and high electromechanical coupling coefficients.

ACKNOWLEDGMENTS

The authors thank the financial support of this research from National Council of ROC through the grant NSC91-2811-E-002-056.

NOMENCLATURE

C_{ijkl} elastic stiffness at constant electric field (N/m^2)
D_i electric displacement vector (C/m^2)
$\overline{D_z}$ amplitude of *z*-component electric displacement (C/m^2)
e_{lij} piezoelectric constant (C/m^2)
f frequency (Hz)
$\boldsymbol{G}$ surface impedance tensor
H thickness of the piezoelectric layer (m)
k_x *x*-component of wave vector (m^{-1})
k_z *z*-component of wave vector (m^{-1})
K_s^2 electromechanical coupling coefficient (%)
$\boldsymbol{N}$ fundamental acoustic tensor
$\overline{\boldsymbol{t}}$ amplitude of stress vector (N/m^2)
$\boldsymbol{T}$ generalized traction vector
u_i mechanical displacement vector (m)
$\overline{\boldsymbol{u}}$ amplitude of mechanical displacement (m)
$\boldsymbol{U}$ generalized displacement vector
v_0 surface wave phase velocity under open-circuited interface condition (m/s)
v_m surface wave phase velocity under short-circuited interface condition (m/s)
$\boldsymbol{Z}_{\alpha j}$ local impedance of *j*th layer
β wave number of v_0 (m^{-1})
ε_{il} dielectric constant at constant strain
ε_s effective permittivity (F/m)
$\varepsilon_s^{(\infty)}$ effective permittivity at infinite slowness (F/m)
λ wavelength (m)
$\overline{\xi}$ state vector
ε_0 permittivity of free space (F/m)
ρ mass density (kg/m^3)
σ_{ij} Cauchy stress tensor (N/m^2)
ϕ electric potential (V)
$\overline{\phi}$ amplitude of electric potential (V)
ω circular frequency (s^{-1})

REFERENCES

Adler, E. L., 1990, "Matrix Methods Applied to Acoustic Waves in Multilayers," *IEEE Transactions on Ultrasonics, Ferroelectrics and Frequency Control*, Vol. 37, No. 6, pp. 485-490.

Adler, E. L, 1994, "SAW and Pseudo-SAW Properties Using Matrix Methods," *IEEE Transactions on Ultrasonics, Ferroelectrics and Frequency Control*, Vol. 41, No. 5, pp. 699-705.

Adler, E. L., and Solie, L., 1995, "ZnO on Diamond: SAWs and Pseudo-SAWs," *Proceedings of the IEEE Ultrasonics Symposium*, Seattle, WA, USA, Vol.1, pp. 341-344.

Fahmy, A. H., and Adler, E. L., 1973, "Propagation of Acoustic Surface Waves in Multilayers: A Matrix Description," *Applied Physics Letters*, Vol. 22, No. 10, pp. 495-497.

Honein, B., Braga, A.M.B., Barbone, P., and Herrmann, G., 1991, "Wave Propagation in Piezoelectric Layered Media with Some Applications," *Journal of*

Intelligent Material Systems and Structures, Vol. 2, No. 4, pp. 542-557.

Ingebrigtsen, K. A., 1969, "Surface Waves in Piezoelectrics," *Journal of Applied Physics*, Vol. 40, pp. 2681-2686.

Ingebrigtsen, K. A., and Tonning, A., 1969, "Elastic Surface Waves in Crystals," *Physical Review*, Vol. 184, No. 3, pp. 942-951.

Matthews, H., 1977, *Surface Wave Filters: Design, Construction, and Use*, Eq. (2.30), pp. 66, Wiley, New York, USA.

Morgan, D. P., 1991, *Surface-Wave Devices for Signal Processing*, Elsevier, New York, USA.

Nakahata, H., Higaki, K., Hachigo, A., Shikata, S., Fukmori, N., Takahashi, Y., Kajihara, T., and Yamamoto, Y., 1994, "High Frequency Surface Acoustic Wave Filter Using ZnO/diamond/Si Structure," J*apanese Journal of Applied Physics, Part 1: Regular Papers & Short Notes & Review Papers*, Vol. 33, No. 1, pp. 324-328.

Nakahata, H., Hachigo, A., Higaki, K., Fujii, S., Shikata, S., and Fujimori, N., 1995, "Theoretical study on SAW Characteristics of Layered Structures Including a Diamond Layer," *IEEE Transactions on Ultrasonics, Ferroelectrics and Frequency Control*, Vol. 42, No. 3, pp. 362-375.

Nakahata, H., Higaki, K., Fujii, S., Hachigo, A., Kitabayashi, H., Tanabe, K., Seki, Y., and Shikata, S., 1995, "SAW Devices on Diamond," *Proceedings of the IEEE Ultrasonics Symposium*, Seattle, WA, USA, pp. 361-370.

Nakahata, H., Kitabayashi, H., Hachigo, A., Higaki, K., Fujii, S., Uemura, T., and Shikata, S., 1998, "Diamond SAW Filter for 2.488 Gbps Retiming, *Proceedings of the IEEE Ultrasonics Symposium*, Sendai, Japan, pp. 319-322.

Stroh, A. N., 1962, "Steady State Problems in Anisotropic Elasticity," *Journal of Mathematics and Physics*, Vol. 41, pp. 77-103.

Wu, T.-T., and Chen, Y.-Y., 2002, "Exact analysis of Dispersive SAW Devices on ZnO/diamond/Si-Layered Structures," *IEEE Transactions on Ultrasonics, Ferroelectrics and Frequency Control*, Vol. 49, No. 1, pp. 142-149.

Yamanouchi, K., Sakuri, N., and Satoh, T., 1989, "SAW Propagation Characteristics and Fabrication Technology of Piezoelectric Thin Film/Diamond Structure," *Proceedings of the IEEE Ultrasonics Symposium*, Montreal, Quebec, Canada, pp. 351-354.

Manuscript Received: Jun. 11, 2004
and Accepted: Jul. 02, 2004